NATIONAL ADVISORY COMMITTEE FOR AERONAUTICS

WARTIME REPORT

ORIGINALLY ISSUED

June 1945 as
Advance Restricted Report L5E10

EVALUATION OF THE INDUCED-VELOCITY FIELD

OF AN IDEALIZED HELICOPTER ROTOR

By Robert P. Coleman, Arnold M. Feingold,
and Carl W. Stempin

Langley Memorial Aeronautical Laboratory
Langley Field, Va.

WASHINGTON

NATIONAL ADVISORY COMMITTEE FOR AERONAUTICS

ADVANCE RESTRICTED REPORT

EVALUATION OF THE INDUCED-VELOCITY FIELD

OF AN IDEALIZED HELICOPTER ROTOR

By Robert P. Coleman, Arnold M. Feingold
and Carl W. Stempin

SUMMARY

The work reported was undertaken in connection with a vibration study of helicopter rotors. The analysis of vibration and certain other problems require a knowledge not only of the average induced velocity but also of its distribution around the rotor disk. A concept of a simplified vortex system of a rotor wake is used in obtaining a formula for the normal component of induced velocity along the fore-and-aft diameter of the rotor disk. This formula is intended to represent the main effect of the skewed wake in producing an uneven velocity pattern at the rotor. This induced velocity is expressed in terms of elliptic integrals as a function of the skew angle and of the circulation per unit axial length of the wake. A simple approximation to this function consisting of the first two terms of a Taylor expansion and giving the value and the slope of the induced-velocity function at the center of the disk is also presented.

An approximate method of representing the induced velocity in terms of flight velocity for a given thrust has also been indicated by combining the present theory with Glauert's thrust equation.

A comparison of the theory with corresponding values of induced velocities computed by Seibel's formula from pitching-moment data published by Wheatley and Bioletti is taken as evidence that the most significant factors have been taken into account.

INTRODUCTION

The work reported herein was undertaken in connection with a vibration study of helicopter rotors. Although for certain purposes the use of an average induced velocity assumed constant over the rotor disk gives reasonable accuracy, the analysis of vibration and certain other problems require a knowledge of the distribution of induced velocity around the rotor disk. Very little such information, however, is available. Several writers have recognized that the induced velocity increases toward the rear of the rotor disk but have left the magnitude of this increase as a matter of speculation. Glauert (reference 1) and Wheatley (reference 2) have used an induced-velocity formula containing a first harmonic term with an unknown coefficient K having a value somewhere between 0 and 1. Nikolsky (reference 3) has suggested a formula that is equivalent to putting $K = 2\mu$, where μ is the ratio of the flight velocity parallel to the disk to the tip speed. Seibel (reference 4) has recently suggested a method of deducing values of the first harmonic induced velocity from experimental measurements of the pitching moment of a gyroplane by Wheatley and Bioletti (reference 5). Seibel gives an example of the use of such data for assumed values of pertinent parameters and shows that the resulting variations of induced drag may be expected to produce a peak of vibration at around 25 miles per hour for a typical case.

In the present paper a concept of a simplified vortex system of a rotor is used for obtaining a formula for the normal component of induced velocity along the fore-and-aft diameter of the rotor disk.

BASIS OF ANALYSIS

The aerodynamic theory of helicopters can be thought of as a generalization of propeller theory; thus certain analytical methods found in propeller literature can be extended to apply to helicopters. The method used herein is based on the assumption of an idealized picture of a wake vortex pattern consisting of an elliptic cylinder which is, in general, skewed with respect to the rotor axis at an angle that depends upon the flight velocity and upon the induced velocities. Enough simplifying

assumptions are made about the wake vorticity distribution to obtain a tractable form for the integration of the Biot and Savart law and thus to represent the main effect of the skewed wake in producing an uneven induced-velocity pattern at the rotor.

The wake pattern is assumed, for the present purpose, to form a continuous distribution of vortex lines on the surface of an elliptic cylinder such as would be formed by the vorticity shed from an infinite number of blades with constant circulation and very light loading. The analysis is further simplified by making use of the property that the induced-velocity field of the helical vortex system can be considered formed from two simpler vortex systems of which one is composed of circular vortex rings and the other of axial vortex lines. (See fig. 1.) The circular rings determine the fore-and-aft distribution of velocities, which are the important ones at small advance ratios; whereas the axial lines determine the rotational velocities of the wake, which are not considered important for the present problem.

With the assumed picture of the vortex wake, the normal component of induced velocity along the fore-and-aft diameter of the rotor disk is obtained in closed form as a function of the wake geometry and of the strength of the vortex sheet.

Although the skew angle and the vortex strength are the fundamental variables of the present problem, it is desirable in applying the theory to have the induced velocity expressed in terms of flight velocity for constant thrust. One method of representing the results in this form has therefore been indicated by combining them with Glauert's thrust equation.

SYMBOLS

χ wake skew angle

ξ, η, ζ coordinates relative to skewed wake (see fig. 2)

x, y, z coordinates relative to rotor disk (see fig. 2)

v_z normal induced-velocity component at rotor disk

$v_x{}'$, $v_z{}'$, $v_\xi{}'$, $v_\zeta{}'$ induced-velocity components in ultimate wake

u value of induced velocity at center of rotor disk

u_1 rate of change of induced velocity along fore-and-aft diameter of rotor at $r = 0$

u_0 hovering induced velocity

V flight velocity

V' resultant velocity at rotor disk in Glauert's formula

α angle of flight path to rotor disk

r distance from hub to position on blade; expressed nondimensionally in terms of rotor radius

ψ azimuth angle of blade position

T thrust

ρ air density

A area of rotor disk

C_T thrust coefficient

dl line element

ANALYSIS

Consider the vortex wake pattern of figure 1(b). Appendix A shows that, if the vortex lines are circles, the induced velocities inside the ultimate wake (see fig. 2) are related by the equation

$$\frac{v_\xi{}'}{v_\zeta{}'} = \tan\frac{\chi}{2} \tag{1}$$

For $\chi > \frac{\pi}{2}$ $\pi - \chi$ must be used in place of χ.

The evaluation of the induced velocity at the disk is given in appendix B. The complete expression for the distribution of the component normal to the disk along the fore-and-aft diameter is

$$\frac{v_z}{v_z{}'} = \frac{1}{2} - \frac{r}{\pi \sin\chi} K(r)$$

$$+ \frac{r(r+1)}{4\pi \tan\chi \sqrt{\tan^2\chi + r^2}} \left[\left(b_1 + j^2\right) \Pi\left(\frac{\pi}{2}, b_1, j\right) + \left(b_2 - j^2\right) \Pi\left(\frac{\pi}{2}, -b_2, j\right) \right]$$

(2)

where

$K(r)$ and $\Pi\left(\frac{\pi}{2}, b_1, j\right)$ are complete elliptic integrals of

the first and third kinds, respectively, and b_1, b_2, and j are defined following equation (B12) in appendix B.

For many purposes a sufficient approximation to this expression is obtained by using the value and the slope of the function at $r = 0$ representing the first two terms of a Taylor expansion

$$v_z = u + u_1 r \cos\psi + \ldots \qquad (3)$$

where, for $\chi < \frac{\pi}{2}$,

$$u_1 = u \tan\frac{\chi}{2}$$

and, for $\chi > \frac{\pi}{2}$,

$$u_1 = u \cot\frac{\chi}{2}$$

That the higher-order terms are small is indicated from the plot of the exact expression for vertical induced velocity against radius for the extreme case in which $\chi = \frac{\pi}{2}$. (See fig. 3.)

In order to make use of the expressions developed herein, the skew angle χ must be related to other flight parameters. A simple method is to combine equation (3) with the expressions given by Wald (reference 6), which are based on Glauert's formula for thrust. The induced velocity u in Glauert's formula

$$T = 2\rho A u V'$$
(4)

is identified with the value at the center of the disk in the present theory.

From the geometry of the wake, it can be seen that

$$\frac{v_\xi'}{V} = \cos(\chi + \alpha)$$
(5)

Then by using the relations, for $\chi < \dfrac{\pi}{2}$,

$$\frac{v_\xi'}{v_\zeta'} = \tan\frac{\chi}{2}$$
(6a)

for $\chi > \dfrac{\pi}{2}$,

$$\frac{v_\xi'}{v_\zeta'} = \cot\frac{\chi}{2}$$
(6b)

and

$$\left. \begin{aligned} u &= \frac{v_z'}{2} \\[2mm] &= \frac{v_\zeta'}{2} \end{aligned} \right\}$$
(7)

it follows that

$$\frac{V}{u} = \frac{2\tan\dfrac{\chi}{2}}{\cos(\chi + \alpha)}$$
(8)

If Wald's equation

$$u^4 + 2u^3 V \sin \alpha + u^2 V^2 = u_o^4 \qquad . \quad (9)$$

is written in the form

$$\left.\begin{array}{c} \left(\dfrac{u}{u_o}\right)^4 = \dfrac{1}{1 + 2\dfrac{V}{u}\sin\alpha + \left(\dfrac{V}{u}\right)^2} \\[3em] \dfrac{V}{u_o} = \dfrac{u}{u_o}\dfrac{V}{u} \end{array}\right\} \qquad (10)$$

equations (3), (8), and (10) can be used to obtain plots of u/u_o and u_1/u_o against V/u_o for constant α. These plots are shown in figure 4. These curves indicate that the first harmonic velocity term is a maximum at a fairly low flight speed, as was expected from Seibel's interpretation of pitching-moment data. The curves also show that the height of the peak decreases as the angle α increases toward 90°, which corresponds to vertical climb of a helicopter.

Curves are also plotted in figure 4 for negative values of α but, since the vortex ring and the turbulent states of operation are included in this range, the vortex theory based on the assumption of a long cylindrical wake cannot be expected to give reliable results. Part of the curves of figure 4 have consequently been plotted as dashed lines to indicate their provisional status.

A direct experimental check of the applicability of the present theory has not been possible because of the unavailability of data on induced velocities. A tentative comparison with Seibel's method has been made, however, by computing the induced velocities corresponding to a series of test conditions for which pitching-moment data are available and then using Seibel's formula to compute values of induced velocity for comparison with the results of the present theory.

A plot of u_1/u_0 against V/u_0, determined by Seibel's formula and the data of reference 5, is shown in figure 5 for two values of the blade pitch setting. For comparison, the formula for u_1/u_0 given in the present paper has been applied $\left(\text{by use of the}\right.$

formula $\left.\dfrac{V}{u_0} = \dfrac{\mu}{\cos\alpha}\sqrt{\dfrac{2}{C_T}}\right)$ to the same test conditions

specified by the values of α, C_T, and μ in reference 5. The resulting curves are also plotted in figure 5, which shows that both methods give peaks of the same general appearance. Systematic errors influencing the magnitude of the theoretical peak may be expected from several sources, which include assumptions of

(1) Vortices shed only at blade tips

(2) No contraction of wake

(3) Infinite number of blades

(4) Slope of induced-velocity function as representative of front and back inequality of velocity

The net effect of these assumptions appears to be to underestimate the magnitude of u_1. The use of an effective radius smaller than the actual rotor radius would give larger induced velocities for the same total thrust and would tend to show closer agreement between the curves.

In view of the various approximations and possible sources of error involved in both methods, the qualitative agreement between these two methods is evidence that the most significant factors have been taken into account. Further testing and refinement of analysis should lead to a more detailed understanding of the phenomena involved.

CONCLUSIONS

From theoretical considerations, it was concluded that the important variable determining the increase of induced velocity toward the rear of a helicopter rotor

in forward flight is the angle χ by which the wake axis is skewed from the rotor disk axis. If the induced-velocity distribution is represented by a series expression of the form

$$v_z = u + u_1 r \cos \psi + \dots$$

integration of the Biot and Savart law for a simplified form of vortex wake gives the value

$$u_1 = u \tan \frac{\chi}{2}$$

where

v_z normal component of induced velocity

u value of v_z at center of disk

r nondimensional radial coordinate

ψ azimuth angle

The exact expression for the normal component of the induced velocity along the fore-and-aft diameter for the assumed vortex wake was also found in closed form in terms of complete elliptic integrals of the first and third kinds.

It is believed that systematic errors due to the use of an idealized wake may be partly compensated by using an effective radius smaller than the actual rotor radius.

Langley Memorial Aeronautical Laboratory
    National Advisory Committee for Aeronautics
       Langley Field, Va.

APPENDIX A

VELOCITIES IN THE ULTIMATE WAKE

The assumption of circular vortex lines on the surface of an elliptic cylinder forming the ultimate wake is shown to imply a velocity which is constant inside the wake and such that

$$\frac{v_\xi{}'}{v_\zeta{}'} = \tan\frac{\chi}{2}$$

The method is first to try to satisfy all the requirements of the problem by assuming that inside the cylinder the velocity components $v_\xi{}'$ and $v_\zeta{}'$ are constant but of undetermined magnitude. Their constancy means that the wake cylinder moves as though it were a rigid cylinder and the flow outside is consequently the same as the well-known velocity field outside a solid cylinder. The vortex strength can then be determined in terms of the assumed velocities by evaluating the line integral of velocity around a suitable path enclosing a portion of the surface of the cylinder and equating this integral to the total circulation of vortex lines that thread the path of integration. This equation yields an expression for the slope of vortex lines on the cylinder, which can be integrated to give an equation of the vortex lines. Comparison with the equation for circles shows that

$$\frac{v_\xi{}'}{v_\zeta{}'} = \tan\frac{\chi}{2}$$

Consider the line integral of velocity around path A of figure 6. If the circulation per unit axial distance along the wake is denoted by Γ/s, the line integral around path A shows that

$$\frac{\Gamma}{s} = v_\zeta{}'$$

Now consider the velocity integral for path B in the $\xi\eta$-plane of figure 6. Referred to axes fixed in still air, the velocity potential on the outside surface for the motions in the $\xi\eta$-plane is

$$\emptyset = -v_\xi' a \cos\theta$$

where v_ξ' refers to the constant velocity inside the cylinder. This potential is the same as in the flow at the surface of an elliptic cylinder moving through an incompressible fluid that is at rest at infinity. Then

$$\int \overline{v} \cdot \overline{dl} = \frac{\partial\emptyset}{\partial\theta} d\theta - v_\xi' \, d\xi'$$

$$= v_\xi' (a + b) \sin\theta \, d\theta$$

This integral is equal to the total circulation threaded at B. If the slope of the vortex lines is represented by $d\xi/d\theta$, the number of lines that thread the path B is

$$\frac{\Gamma}{s} \frac{d\xi}{d\theta} \, d\theta$$

Consequently

$$\frac{\Gamma}{s} \frac{d\xi}{d\theta} = v_\xi' (a + b) \sin\theta$$

and, after integration, this equation becomes

$$\xi = -\frac{v_\xi' s}{\Gamma} (a + b) \cos\theta$$

The equation of a circular vortex line, however, is

$$\xi = -c \cos\theta$$

where

$$c = \sqrt{a^2 - b^2}$$

Hence,

$$\frac{v_\xi' s}{\Gamma} = \frac{v_\xi'}{v_\zeta'} = \frac{c}{a + b}$$

$$= \frac{\sin \chi}{1 + \cos \chi}$$

$$= \tan \frac{\chi}{2}$$

It should be noted that this relation implies that, inside the ultimate-wake cylinder,

$$v_z' = v_\zeta'$$

APPENDIX B

INDUCED-VELOCITY FIELD AT ROTOR DISK

As stated previously, the entire vortex wake is considered to be an elliptic cylinder composed of a continuous distribution of circular vortex filaments parallel to the rotor disk. (See fig. 7.) By using the Biot and Savart law, the velocity vector induced by the vortex wake at any point P having coordinates (r, ψ) in the plane of the rotor disk is given by

$$\bar{v} = \frac{\Gamma}{s} \frac{\sqrt{1+m^2}}{4\pi} \int_{\theta=0}^{2\pi} \int_{z=0}^{\infty} \begin{vmatrix} \bar{i} & \bar{j} & \bar{k} \\ r\cos\psi + \cos\theta - z\tan\chi & -\sin\theta - r\sin\psi & z \\ \sin\theta & \cos\theta & 0 \end{vmatrix} \frac{dz\,d\theta}{\rho^3}$$

(B1)

where

Γ/s axial-vortex strength

r nondimensional distance in terms of rotor radius

$m = \tan\chi$

$\bar{i}, \bar{j}, \bar{k}$ unit vectors along x, y, and z directions, respectively

ρ distance from point (r, ψ) to element $d\theta$ dz of wake surface

The value of ρ is given by

$$\rho^2 = 1 + r^2 + z^2(1+m^2) - 2rzm\cos\psi - 2zm\cos\theta + 2r\cos(\psi - \theta)$$

(B2)

The vertical component of the induced velocity v_z at the point (r, ψ) can be written from equation (B1) as

$$v_z = \frac{\Gamma}{s}\frac{\sqrt{1+m^2}}{4\pi}\int_{\theta=0}^{2\pi}\int_{z=0}^{\infty}\frac{1 - zm\cos\theta + r\cos(\psi - \theta)}{\rho^3}\,dz\,d\theta \qquad (B3)$$

The value of v_z along the fore-and-aft diameter of the rotor disk can be determined by setting $\psi = \pi$ in equations (B2) and (B3); thus

$$v_{z_{\psi=\pi}} = v_z'\frac{\sqrt{1+m^2}}{4\pi}\int_{\theta=0}^{2\pi}\int_{z=0}^{\infty}\frac{[1 - (zm + r)\cos\theta]\,dz\,d\theta}{\left[1 + r^2 + z^2(1+m^2) + 2rzm - 2(mz + r)\cos\theta\right]^{3/2}}$$
$$(B4)$$

where Γ/s has been replaced by the vertical induced velocity in the ultimate wake v_z'. (See appendix A.) The integration with respect to z can be readily performed by use of formula 200 of Peirce's "A Short Table of Integrals." The result is

$$v_{z_{\psi=\pi}} = \frac{v_z'}{2\pi}\int_{\theta=0}^{\pi}\left[1 + \frac{r\cos\theta - r^2}{1 + r^2 - 2r\cos\theta + m^2\sin^2\theta} - \frac{r\sqrt{1+m^2}}{m\sqrt{1+r^2 - 2r\cos\theta}}\right.$$

$$\left. + \frac{r\sqrt{1+m^2}\,\sqrt{1 - 2r\cos\theta + r^2}}{m\left(1 + r^2 - 2r\cos\theta + m^2\sin^2\theta\right)}\right]d\theta \qquad (B5)$$

in which the limits have been changed to 0 to π since the integrand is an even function of θ.

The value of r is assumed to be positive in the integrations. For negative values of r, the substitution $\theta = \pi - \emptyset$ converts the integral into one similar to the integral for positive values of r. The integral of the second term of equation (B5) is shown later to be identically zero for all values of $|r| < 1$. It can

then be seen that u, which is the average value
of v_z across the fore-and-aft diameter, is equal to
the value of v_z at the center of the rotor disk since
the curve of v_z against r is symmetric about $r = 0$.
If r is put equal to zero in equation (B5),

$$\left. \begin{aligned} v_{z}{}_{r=0} &= u \\[2mm] &= \frac{v_z{}'}{2} \end{aligned} \right\} \tag{B6}$$

The rate of change of v_z along the fore-and-aft
diameter can be immediately found from equation (B5) by
differentiating within the integral sign (this
differentiation is permissible since the denominators
are always greater than zero for $|r| < 1$), setting
$r = 0$, and then evaluating the resultant integrals. The
result is

$$\begin{aligned} \frac{d v_{z}{}_{\psi=\pi}}{dr} \Bigg]_{r=0} &= -u_1 \\[3mm] &= -\frac{v_z{}'}{2} \frac{\sqrt{1+m^2}}{m} \left(1 - \frac{1}{\pi} \int_{\theta=0}^{\pi} \frac{d\theta}{1 + m^2 \sin^2\theta} \right) \\[3mm] &= -\frac{v_z{}'}{2} \frac{\sqrt{1+m^2}}{m} \left(1 - \frac{1}{\sqrt{1+m^2}} \right) \\[3mm] &= -\frac{v_z{}'}{2} \tan \frac{\chi}{2} \end{aligned} \tag{B7}$$

and from equation (B6)

$$u_1 = u \tan \frac{\chi}{2} \tag{B8}$$

The complete evaluation of equation (B5) is performed most readily by integrating each term separately. The integration is restricted to the case of $|r| < 1$, that is, within the rotor disk.

The integral of the first term of equation (B5) is evidently π.

It is now shown that the integral of the second term of equation (B5) is identically zero. By using the conventional transformation $\tan \frac{\theta}{2} = z$, the integral becomes

$$r \int_{\theta=0}^{\pi} \frac{(\cos \theta - r)d\theta}{1 + r^2 - 2r \cos \theta + m^2 \sin^2 \theta} = 2r \int_{z=0}^{\infty} \frac{\left[1 - z^2 - r\left(1 + z^2\right)\right] dz}{\left(1 + r^2\right)\left(1 + z^2\right)^2 - 2r\left(1 - z^4\right) + 4m^2 z^2}$$

$$(B9)$$

The integrand is finite everywhere, approaches zero as z becomes infinite, and is zero and changes sign only at the point $z^2 = \frac{1 - r}{1 + r}$. Divide the integral into two parts:

$$\int_{z=0}^{\infty} (\ ) \, dz = \int_{z=0}^{\sqrt{\frac{1-r}{1+r}}} (\ ) \, dz + \int_{z=\sqrt{\frac{1-r}{1+r}}}^{\infty} (\ ) \, dz \qquad (B10)$$

If the transformation $z = \frac{1 - r}{1 + r} \frac{1}{w}$ is applied to the second integral of the right-hand side of equation (B10), this integral is seen to be identically equal to the negative of the first integral. The total integral of equation (B10), or equation (B9), thus is zero. This integral is not zero, however, if $|r| > 1$.

The integral of the third term of equation (B5) is equal to

$$-\frac{r\sqrt{1+m^2}}{m}\int_{\theta=0}^{\pi}\frac{d\theta}{\sqrt{1+r^2-2r\cos\theta}} = -\frac{2r\sqrt{1+m^2}}{m}K(r)$$

where $K(r)$ is the complete elliptic integral of the first kind.

The integral of the last term of equation (B5) is evaluated by first using the substitution $\tan\frac{\theta}{2} = z$, then separating into partial fractions, and thus obtaining

$$\frac{r}{m}\sqrt{1+m^2}\int_{\theta=0}^{\pi}\frac{\sqrt{1-2r\cos\theta+r^2}}{1-2r\cos\theta+r^2+m^2\sin^2\theta}\,d\theta$$

$$= \frac{r(1+r)}{2m\sqrt{m^2+r^2}}\int_{z=0}^{\infty}\left[-\frac{\sqrt{\left(1+z^2\right)\left(k^2+z^2\right)}}{z^2+m_1^2}+\frac{\sqrt{\left(1+z^2\right)\left(k^2+z^2\right)}}{z^2+m_2^2}\right]dz$$

$$(B11)$$

where

$$k^2 = \left(\frac{1-r}{1+r}\right)^2$$

$$m_1 = \frac{\sqrt{m^2+1}+\sqrt{m^2+r^2}}{r+1}$$

$$m_2 = \frac{\sqrt{m^2+1}-\sqrt{m^2+r^2}}{r+1}$$

It is noted that $m_1 > 1$ and $m_2 < 1$ for all positive
values of r less than 1. By using the substitution
$z^2 + 1 = \dfrac{1}{y^2}$, the integral of equation (B11) is trans-
formed into the following form after again being
separated into partial fractions:

$$\frac{r(r+1)}{2m\sqrt{m^2+r^2}} \int_{y=0}^{1} \left[\frac{b_1\sqrt{1-j^2y^2}}{\left(1+b_1y^2\right)\sqrt{1-y^2}} + \frac{b_2\sqrt{1-j^2y^2}}{\left(1-b_2y^2\right)\sqrt{1-y^2}} \right] dy \quad (B12)$$

where $b_1 = m_1^2 - 1$, $b_2 = 1 - m_2^2$, and $j^2 = 1 - k^2$.
Integral (B12) is immediately transformed into complete
elliptic integrals of the third kind by multiplying the
numerators and denominators by $\sqrt{1-j^2y^2}$ and separating
into elliptic integrals of the third kind.

By collecting the various integrals, the complete
evaluation of $v_{z_{\psi=\pi}}$ for positive values of r is

$$\frac{v_z}{v_z{}'} = \frac{1}{2} - \frac{r}{\pi \sin\chi} K(r)$$

$$+ \frac{r(r+1)}{4\pi \tan\chi \sqrt{\tan^2\chi + r^2}} \left[\left(b_1 + j^2\right) \Pi\!\left(\frac{\pi}{2}, b_1, j\right) + \left(b_2 - j^2\right) \Pi\!\left(\frac{\pi}{2}, -b_2, j\right) \right] \quad (B13)$$

For negative values of r, the sign of the second
and third terms of equation (B13) should be changed and
r should be considered a positive number throughout the
resultant formula.

REFERENCES

1. Glauert, H.: A General Theory of the Autogyro.
   P. & M. No. 1111, British A.R.C., 1928.

2. Wheatley, John B.: An Aerodynamic Analysis of the
   Autogiro Rotor with a Comparison between
   Calculated and Experimental Results. NACA
   Rep. No. 487, 1934.

3. Nikolsky, Alexander A.: Notes on Helicopter Design
   Theory. Princeton Univ. Press, 1944, p. 97.

4. Seibel, Charles: Periodic Aerodynamic Forces on
   Rotors in Forward Flight. Jour. Aero. Sci.,
   vol. 11, no. 4, Oct. 1944, pp. 339-342.

5. Wheatley, John B., and Bioletti, Carlton: Wind-
   Tunnel Tests of a 10-Foot-Diameter Gyroplane
   Rotor. NACA Rep. No. 536, 1935.

6. Wald, Quentin: A Method for Rapid Estimation of
   Helicopter Performance. Jour. Aero. Sci., vol. 10,
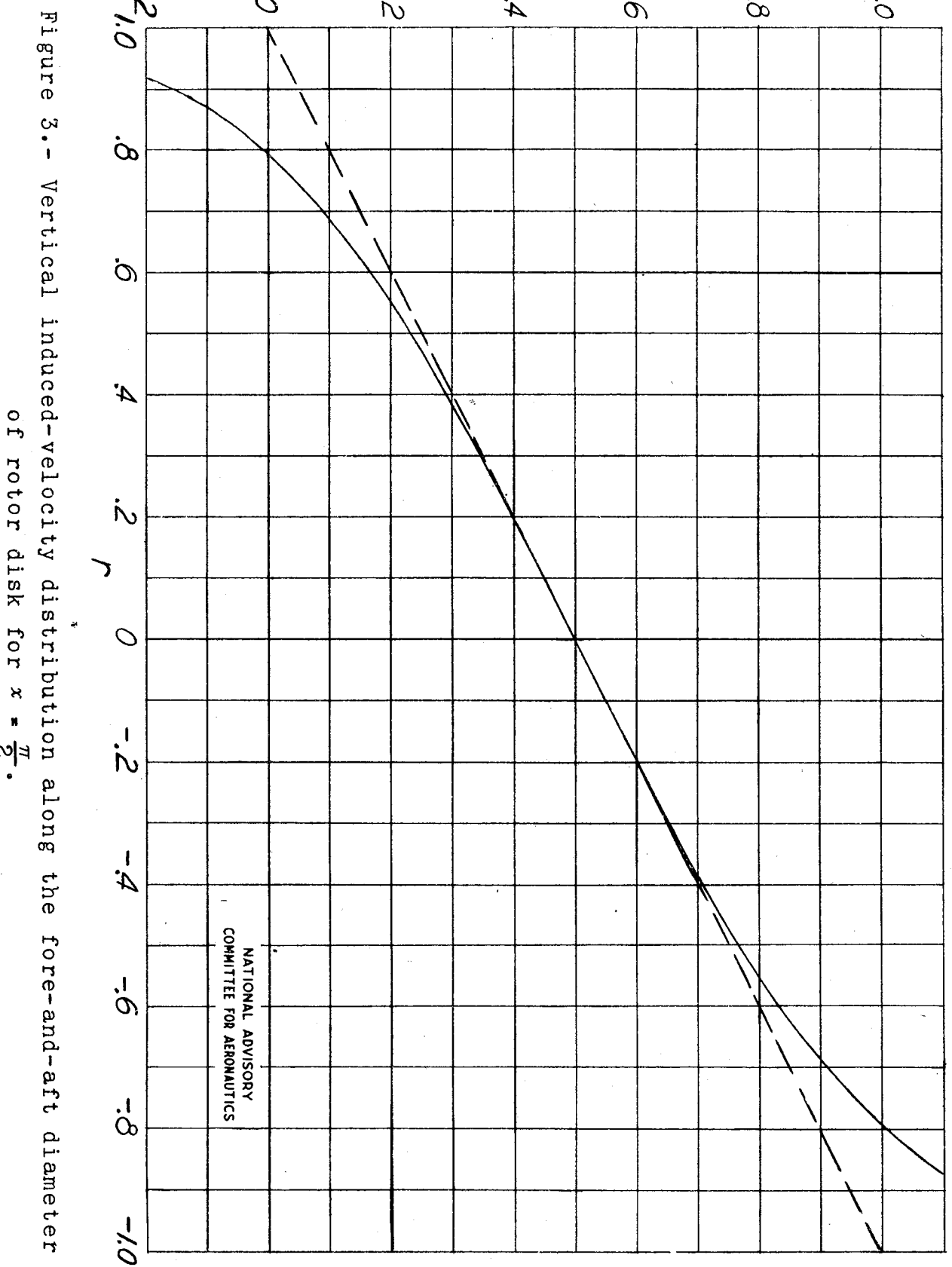   no. 4, April 1943, pp. 131-135.

(a)   (b)   (c)
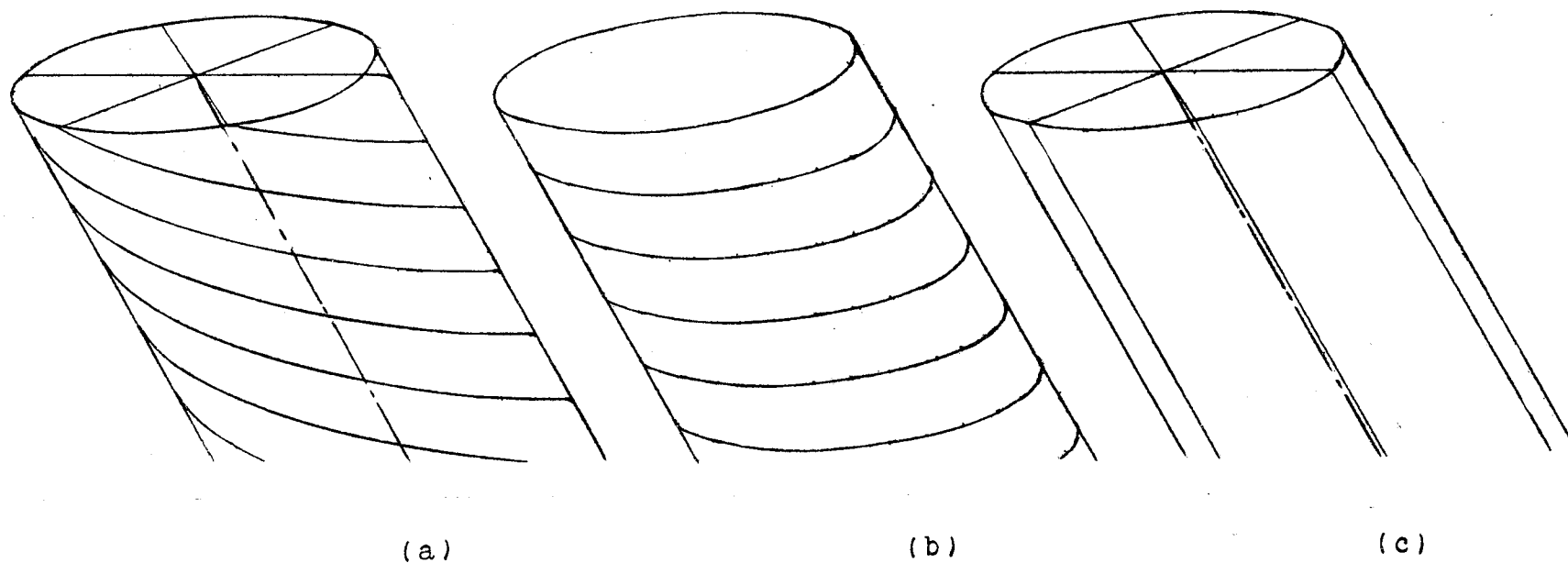
Figure 1.- Representation of skewed helical vortex wake by circular and linear vortex wakes.
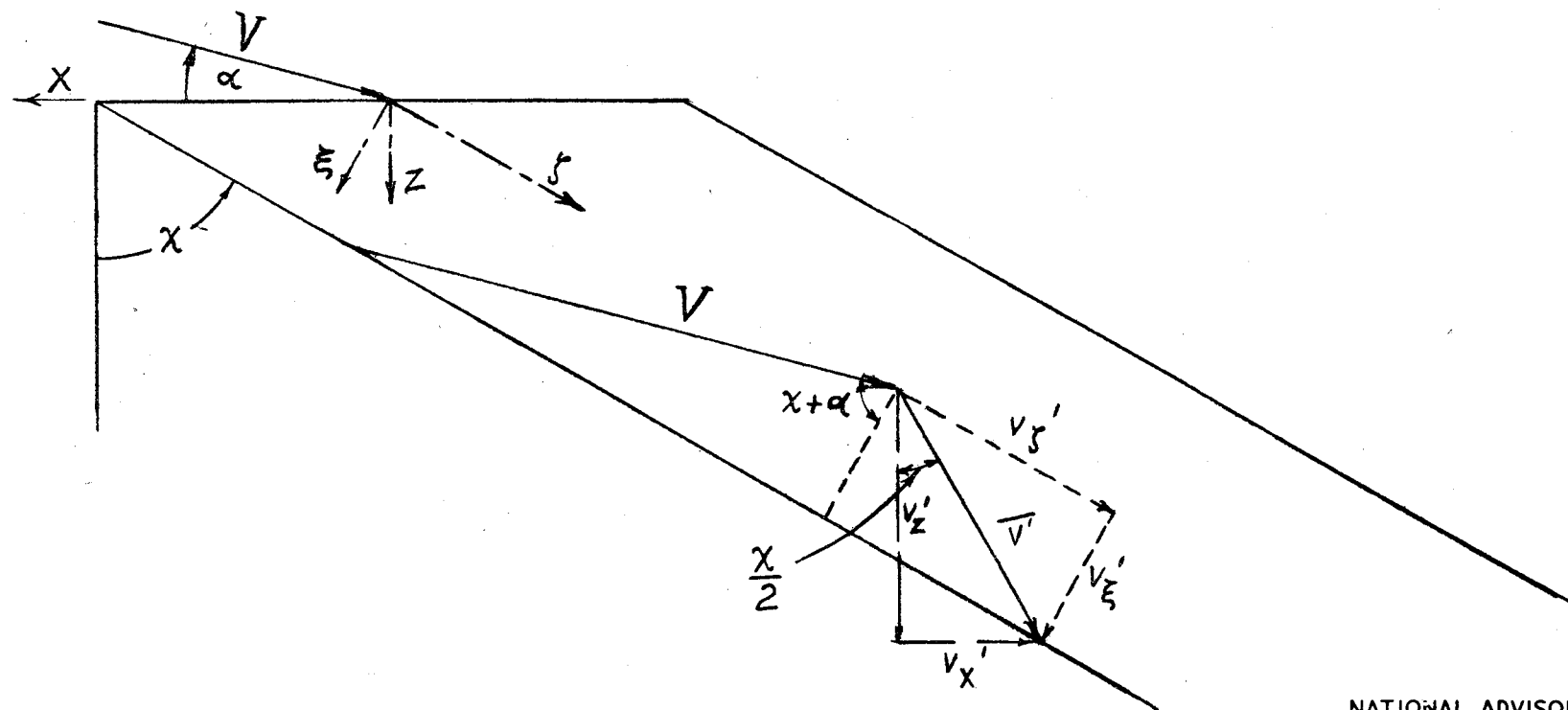
Figure 2.- Axes and velocity components of wake.

Fig. 2

Figure 3.— Vertical induced-velocity distribution along the fore-and-aft diameter of rotor disk for $x = \frac{\pi}{2}$.

NATIONAL ADVISORY
COMMITTEE FOR AERONAUTICS

Fig. 3
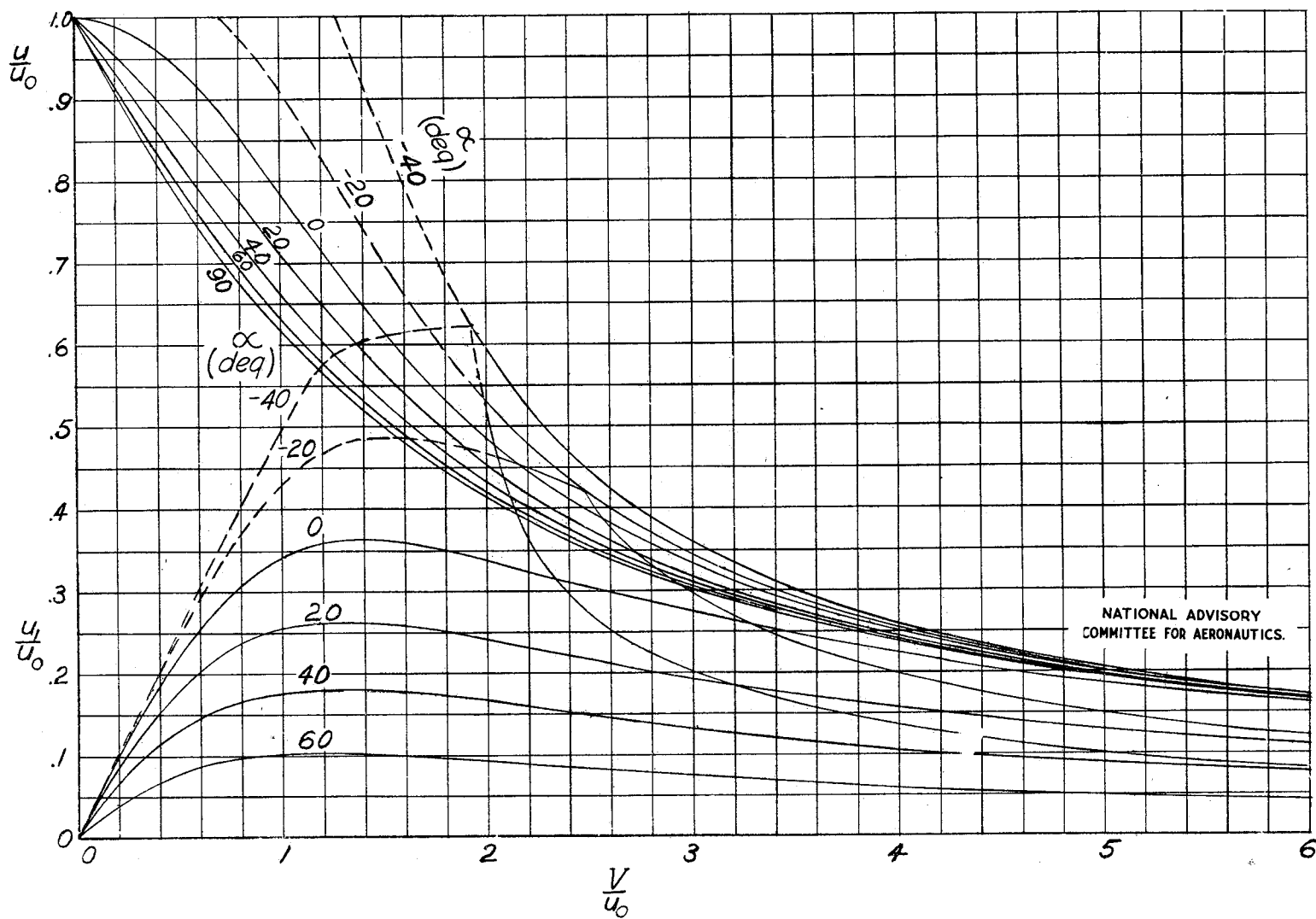
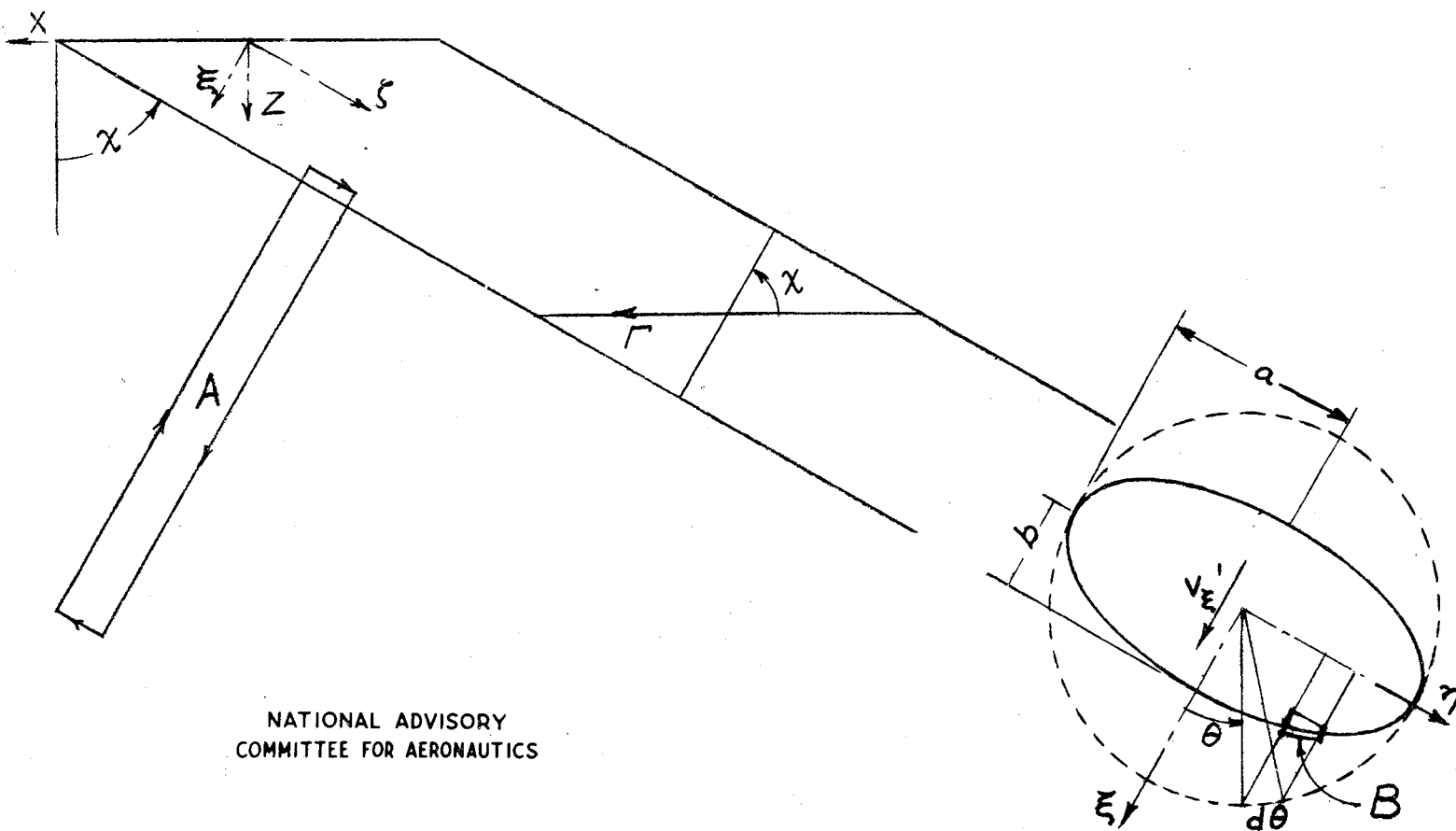Figure 4.- Induced velocities $\frac{u}{u_o}$ and $\frac{u_1}{u_o}$ against flight speed $\frac{V}{u_o}$.

Fig. 4
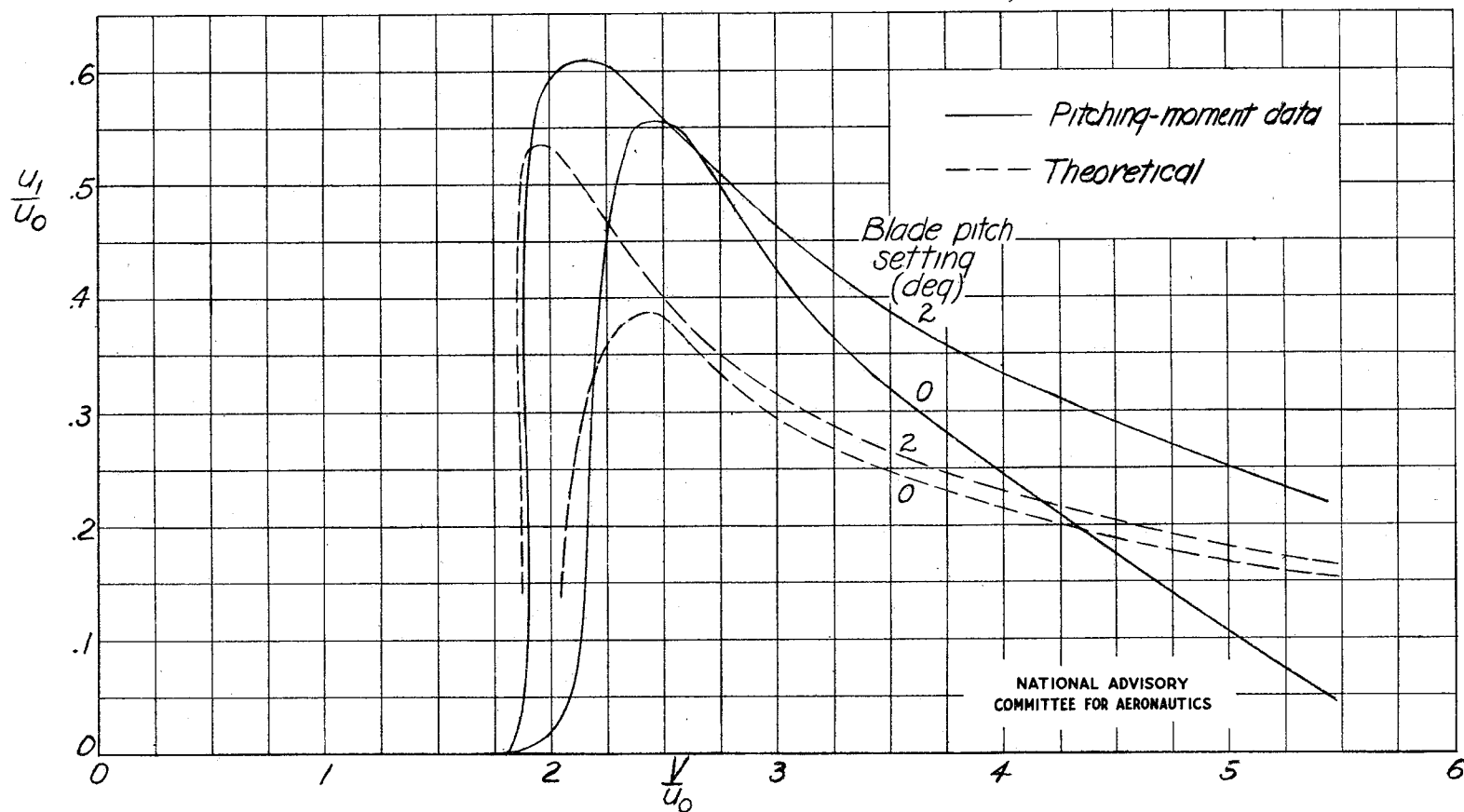
Figure 5.- Comparison of theoretical induced velocities with values deduced from pitching-moment data of reference 5.

Fig. 5

Figure 6.- Integration paths A and B of wake.

Fig. 6
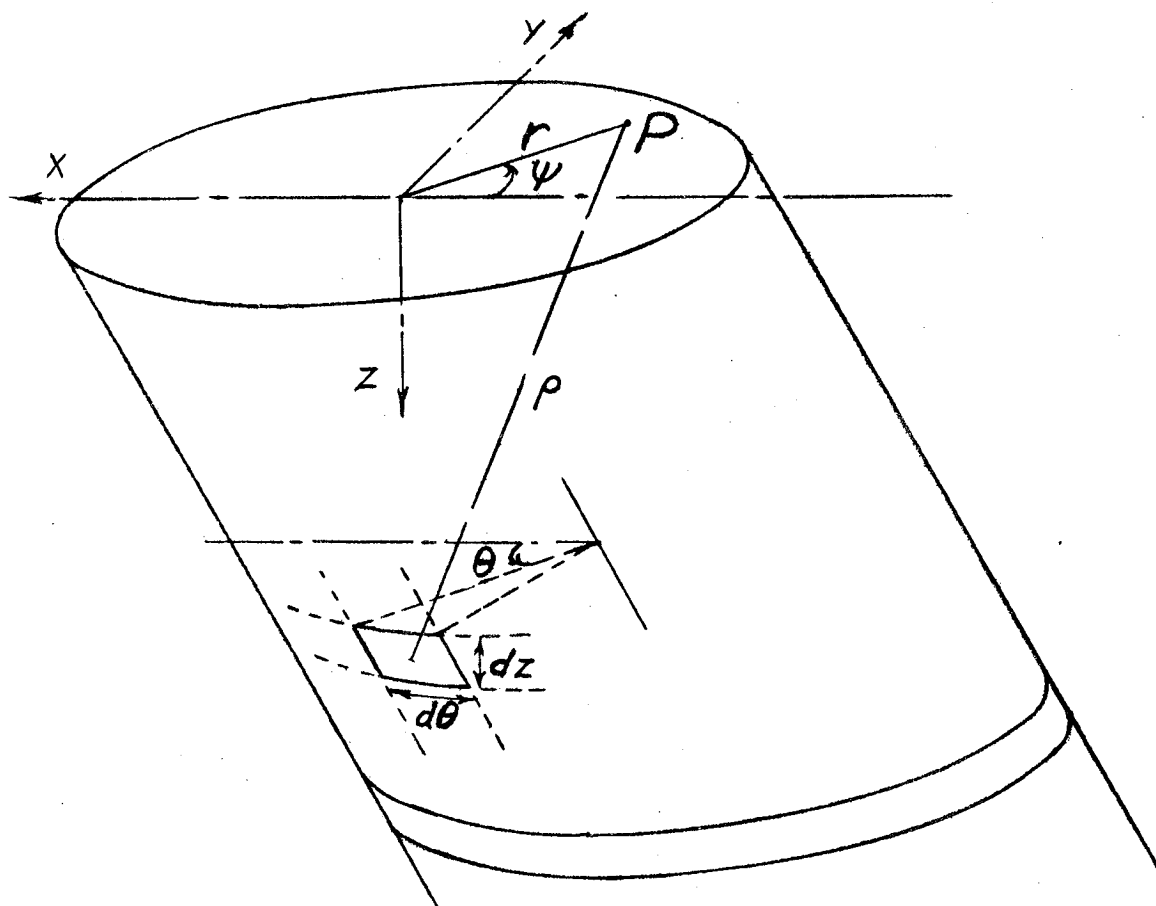
Figure 7.- Coordinate system for obtaining induced
velocities at rotor disk.